



Parametric Finite Element Evaluation of RC Beam-Column Joints

Seyed Ahmad Nezami ^{1*}, Jalil Shafaei ²

^{1*} MSc Student, Faculty of civil Engineering, Shahrood University of Technology, Shahrood, Iran

(s.ahmad.nezami@shahroodut.ac.ir)

² Assistant professor, Faculty of civil Engineering, Shahrood University of Technology, Shahrood, Iran

(Date of received: 04/12/2020, Date of accepted: 15/03/2021)

ABSTRACT

Beam-column connections with non-seismic detailing in buildings with moment resisting lateral load bearing systems, are the major cause of post-earthquake damage. The optimal shape and energy absorption of the moment frame structure is dependent on the design and perfect execution of the beam-column connections. In the beam-column connections, the lack of positive reinforcement of the beam in the joint area and non-extension of the column stirrup in the joint area are common defects of the joints in accordance with new regulations. In this study, finite element models with seismic and non-seismic detail were considered and validate with laboratory tests by considering sliding effect of longitudinal beam reinforcement using modified steel stress-strain curve. Then, the effect of different lateral beam conditions around the joint was considered. The results showed well that the finite element model is more consistent with the experimental results when considering the slip effects of the longitudinal beam reinforcement. Also comparing the results of the models with the different lateral beam conditions showed that confining the non-seismic joints can increase the joint strength against lateral loads.

Keywords:

Reinforced concrete structures, beam-column connection, finite element modeling, bond-slip, monotonic loading.



1. Introduction

Beam–column connections in reinforced concrete (RC) structures play an important role when the frame is subjected to seismic loading. The overall stability of the structure and the formation of the optimal energy absorption mechanism in the beam plastic hinge zone depends on the role of the beam-column joints. The non-seismic detailing in the joint panel area can cause a partial or total collapse of the structure [1]. As shown in Figure 1 the failure of non-seismically detailed beam-column joint can cause to building collapse.



Figure 1. Collapse of the reinforced concrete buildings due to the failure of beam-column connections in recent earthquake (12 November 2017) in Kermanshah-Iran with magnitude of 7.3.

Researchers have provided a lot of experimental studies on beam–column connections, while experimental studies are usually costly and time consuming, and can be restricted by the test facilities and space [2]. The behaviour of the RC beam–column joint is very complex and several parameters such as axial load ratio, reinforcement detailing, concrete strength have significant influences on its seismic performance. It is impractical to fully investigate all parameters through a limited number of experimental tests [3]. Finite element modelling using ABAQUS software platform can provide an opportunity to study the various parameters governing the monotonic behavior of the beam–column joints. The nonlinear compressive and tensile behavior of concrete with steel is the most challenging aspect of finite element modeling of concrete structures. In this study, at the first step, finite element analytical models of beam-column joint are validated with experimentally tested specimens at laboratory to investigate the slip of beam longitudinal reinforcement in the joint panel and the effects of transverse beam connected to the joint panel was analytically investigated. After verification of finite element analytical model, a parametric analysis of beam-column joint by considering of the concrete dilation angle parameter and other parameter affected the performance of joint panel was presented.

2. Finite Element Simulations

In order to evaluate different conditions such as seismic defects, side beam and slip effect of longitudinal reinforcement, 12 numerical models were considered in the finite element software to compare and investigated (Table 1). The numerical models were considered in full accordance with the laboratory samples of Shafaei et al. [4]. The analytical models constructed of reinforced concrete beam-column joints are divided into three categories based on the seismic details and the conventional non-seismic details of the previous construction. According to Figure 2 the first



specimen was considered with seismic details that, by the standards, had sufficient bracing in the junction of the beam longitudinal reinforcement (C1). Non-seismic detail samples (which cover most of the existing joints) include the lack of column hoop in the joint area (C2), and in the latter case, in addition to the previous weakness, no positive beam reinforcement was found in the joint area (C3).

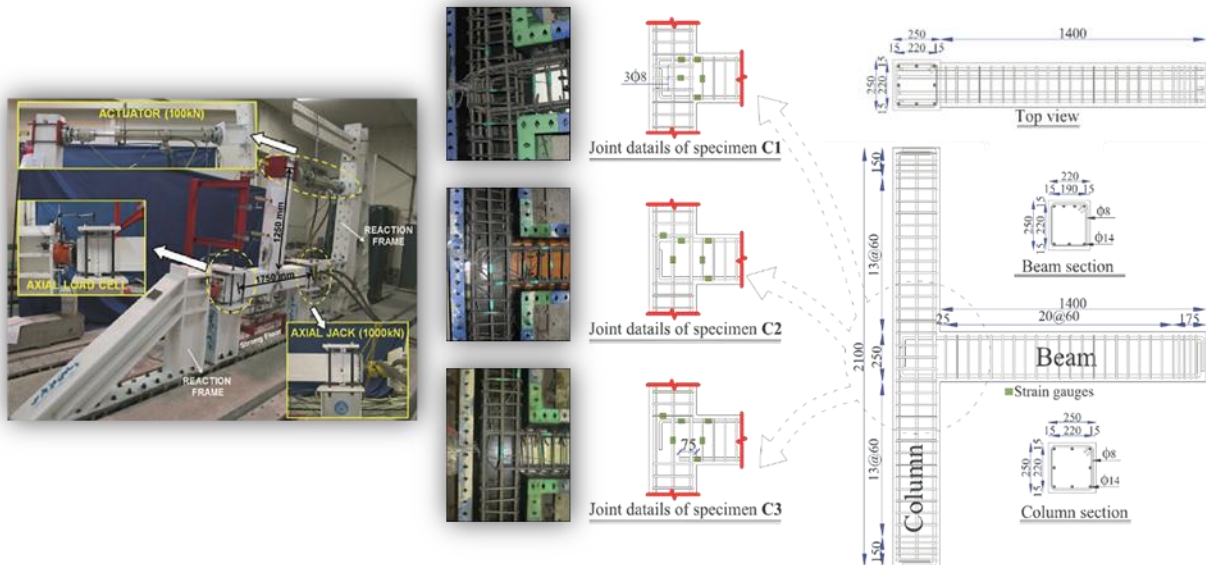


Figure 2. Dimensions and reinforcement details of specimens C1, C2, and C3 (dimensions in millimeters).

Table 1. Nomenclature for simulated specimens.

Model		Reinforcement details type	Conditions of the lateral beam	Bond-slip effects	Loading
No.	ID				
1	C1-1	C1	Exterior joint	–	Monotonic
2	C2-1	C2	Exterior joint	–	Monotonic
3	C3-1	C3	Exterior joint	–	Monotonic
4	C1-1-S	C1	Exterior joint	✓	Monotonic
5	C1-2-S	C1	Corner joint	✓	Monotonic
6	C1-3-S	C1	Exterior middle joint	✓	Monotonic
7	C2-1-S	C2	Exterior joint	✓	Monotonic
8	C2-2-S	C2	Corner joint	✓	Monotonic
9	C2-3-S	C2	Exterior middle joint	✓	Monotonic
10	C3-1-S	C3	Exterior joint	✓	Monotonic
11	C3-2-S	C3	Corner joint	✓	Monotonic
12	C3-3-S	C3	Exterior middle joint	✓	Monotonic

Considering the seismic provisions in the joint panel area enables the concrete core to achieve special confinement conditions. Such confinement significantly increases the strength and ductility of core concrete [5]. The concrete core of the joint panel zone is considered as enclosed in C1 specimens and the modified stress-strain behavior is assumed to be based on (Mander et al., 1988) [5] relationships (Table 2). The mechanical properties of concrete and steel used in the samples are presented in Table 2.



Table 1. Mechanical properties of concrete and reinforcement bars.

Materials	Specimen	Prism compressive strength (MPa)		Prism tensile strength (MPa)	Elastic modulus (MPa)
concrete	C1	23.0		3.0	22540
	C2	23.3		3.0	22687
	C3	24.7		3.1	23500
	C _{core}	45		3.1	23500
	Bar diameter (mm)	Yield strength (MPa)	Ultimate strength (MPa)	Yield strain (%)	Ultimate strain (%)
Steel	8 (ASTM A615G40)	350	410	0.18	18
	14 (ASTM A615G60)	460	680	0.20	13

In this paper, CDP models were used for 3D modeling of reinforced concrete beam-to-column connection in the ABAQUS FE software program. Damage parameters are presented in the CDP model for tensile and compressive stresses as shown in Figure 4. Accordingly, concrete damage occurs only in the softening zone [6]. Also the amount of damage at the moment of final strain of concrete was assumed to be 0.97. Furthermore, the other parameters required in the concrete plastic damage model are outlined in Table 3.

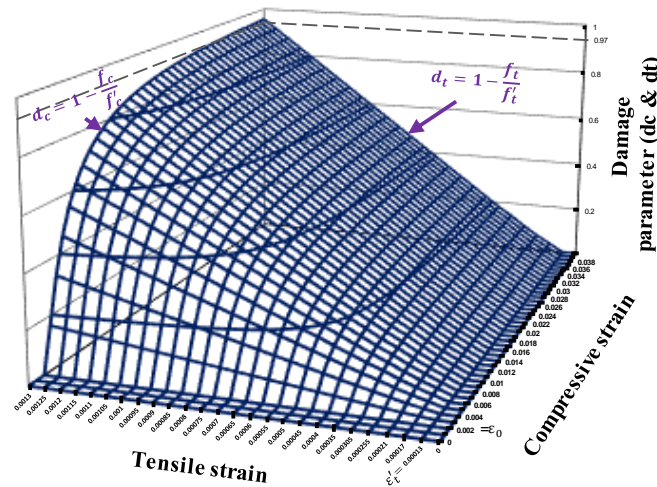


Figure 3. Damage parameters in the CDP model in tension and compression.

Table 2. Parameters for concrete damage plasticity model.

Dilation Angle	Eccentricity	f_{b0} / f_{c0}	k_c	Viscosity Parameter
25	0.1	1.16	0.667	0.001- 0.01



To investigate the effects of the presence and absence of transverse beams on the side of the joints, three selected specimens are expanded to 9 specimens. As shown in Figure 3, it includes the corner connection and the middle side connection.

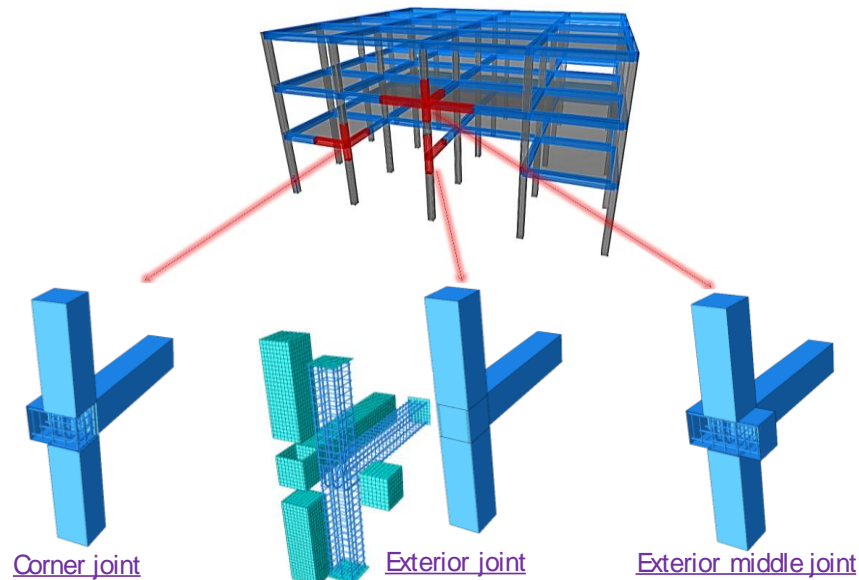


Figure 4. Different conditions of the lateral beam in numerical models.

The effect of reinforcement slip on the beam-column joint area is a very important factor in the seismic behavior of joint [7]. When simulating reinforcement slip directly, using friction modeling between reinforced concrete elements, it is true that the approach is accurate but requires a very complex preprocessing step and significantly increases the cost of computation. Therefore, the rationality of using indirect methods to numerically simulate the effects of reinforcement slip. In recent years, indirect methods with fiber elements and numerical modeling have been performed at the macro level to investigate the effects of reinforcement slip [8- 10]. Most of these methods are assumed to be of sufficient accuracy for considering the reinforcement slip of the beam-to-column connection area, assuming sufficient elongation. According to studies by Feng [11] for indirect simulation of the effects of reinforcing slip on the jointing area, the reinforcement slip can model using modified uniaxial strain stress modeling method which can easily be used in three-dimensional element analysis. Based on the modified strain curve of the reinforcement (Figure 5), a new behavior of the model can be obtained by calculating the modified elasticity modulus of E_s steel and the adjusted final strain of ϵ_u' steel to obtain the effects of sliding reinforcement. The modified values used for modeling in terms of the effect of reinforcement slip on the jointing area are given in Table 4.

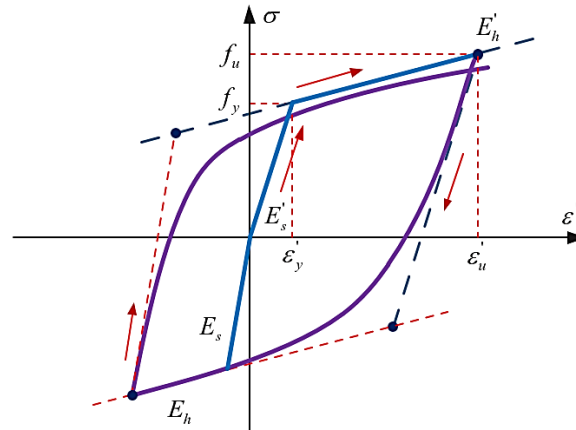


Figure 2. Modified stress-strain relation considering bond-slip for reinforcement bars.

Table 3. Modified parameters considering bond-slip for reinforcement bars.

Parameters	E'_s (Mpa)	b	E'_h (Mpa)	ϵ'_u
All specimens	133334	0.01	1339.4	0.16

3. Results and Discussions

3.1. Comparison of Nonlinear FEA Predictions with Experimental Results

In Figure 6, load-displacement curves calculated from finite element analysis using ABAQUS and laboratory analysis are presented. For better comparison, three specimens C1-1, C2-1, C3-1 as well as similar specimens considering the effect of reinforcement slip (C1-1-S, C2-1-S and C3-1-S) Along with similar laboratory samples was presented in the one graph. As shown in (Figure 6) in the elastic part of the cross-section, the finite element models are more rigid than the laboratory samples. Considering the effect of reinforcement slip in the modeling according to Table 5, it is more consistent with the experimental results (elastic load-displacement slope for laboratory model C1, model C1-1 and model C1-1-S is (2.8, 2.8, and 2.2 respectively)). On average, considering the slip effect with the proposed method results in a 28% greater fit than the case without considering the slip effect in the modeling. This further compatibility illustrates the weakness of ABAQUS software in detecting the effect of sliding armature. The cracking load in all three curves for each model with error percentage is specified in Table 5. As the reinforcement slips, after the friction between the concrete and the reinforcement is reduced, the concrete gradually crumbles and the hardness of the cross section decreases. After cracking, the cracks increase as the load increases and the concrete enters the nonlinear area with increasing cracks width. At this stage, the cross section modeled with finite element method shows greater flexural hardness than the experimental model. Further adaptation of the finite element model to the slip effect to the laboratory model illustrates the successful simulation of the slip effect of the reinforcement.

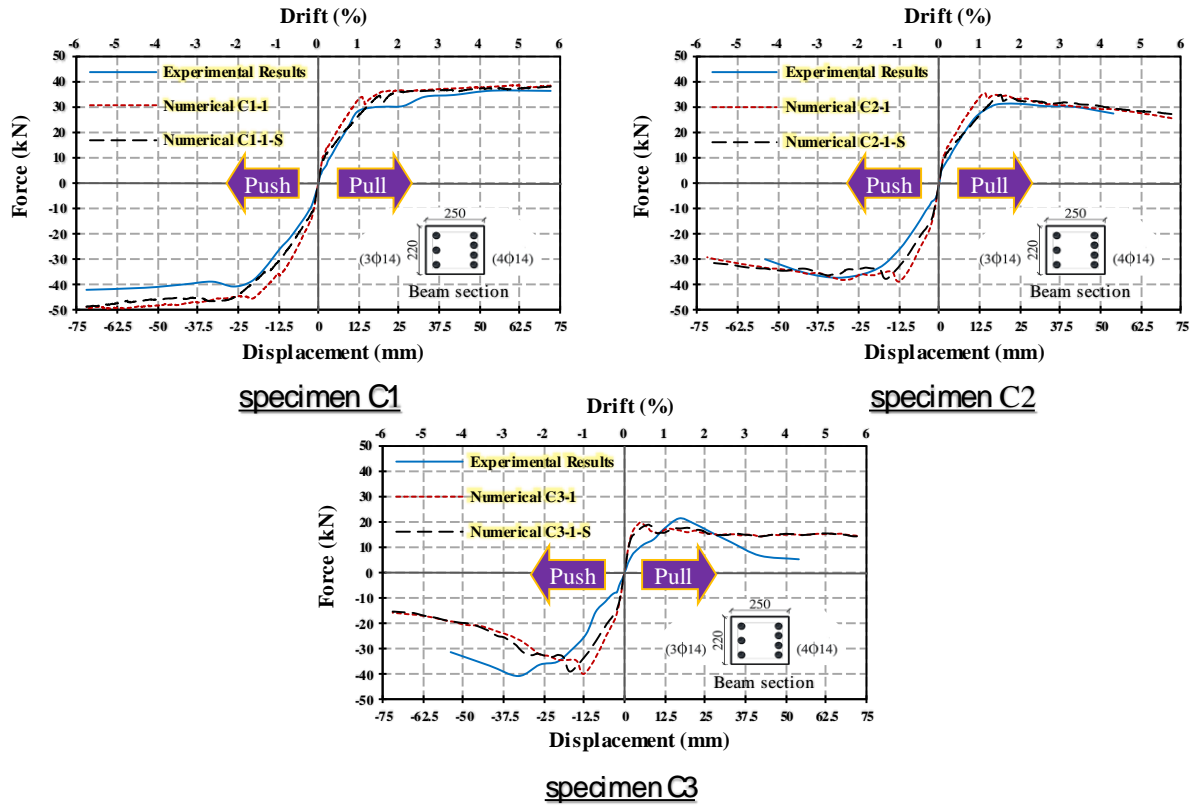


Figure 6. Load-displacement curves calculated from monotonic finite element analysis using ABAQUS and laboratory results.

In model C1, due to the seismic requirements of the joint, the longitudinal reinforcement yields at the face of the joint and thus the plastic hinge is formed for the first time in this area. The plastic behavior of joint is similar in all three curves with the desired energy absorption when forming the plastic joint in the beam, leading to the growth of the beam tensile cracks. According to Table 6, the maximum load tolerable by coupling in the laboratory model, the numerical model C1-1 and the numerical model C1-1-S in the positive direction (pull) are 36.4 kN, 38.55 kN and 37.99 kN, respectively. This occurs in the corresponding displacements of 33/17mm, 13/33mm and 17/33mm respectively, and the amount of ductility obtained in this respect is 4.2, 5.4 and 4.2, respectively. The numerical errors with the laboratory model are 17.7% and 4% for the C1-1 and C1-1-S models, respectively. According to Figure 7, the final similar damage pattern in the analytical model and experimental model can be seen. In specimen C2, due to the weakness of joint in the extension of the column hoop in the joint panel, the shear capacity of the joint is reduced and before the plastic hinge is formed in the beam, the diagonal cracks in the joint panel area appeared. The plastic behavior of joint was similar in all three curves and showed all three brittle fractures with reduced energy absorption. The final load-displacement of all three specimens is in good agreement (Table 5). Figure 7 shows the failure of the joint area in the numerical and laboratory models. In the specimen C3, the lack of positive reinforcement of the beam in addition to the absence of the column hoop in the joint area results in faster sliding of the reinforcement at lower loads, with a severe loss of energy absorption before the plastic hinge is formed in the beam. The maximum load



capacity, displacement such as initiation of joint failures, and ductility value for all numerical specimens are given in Table 5. Figure 7 shows the extension of failure to the joint area. It also observed that failure in the joint area did not allow the reinforcement to reach the maximum capacity and experienced plastic hinge.

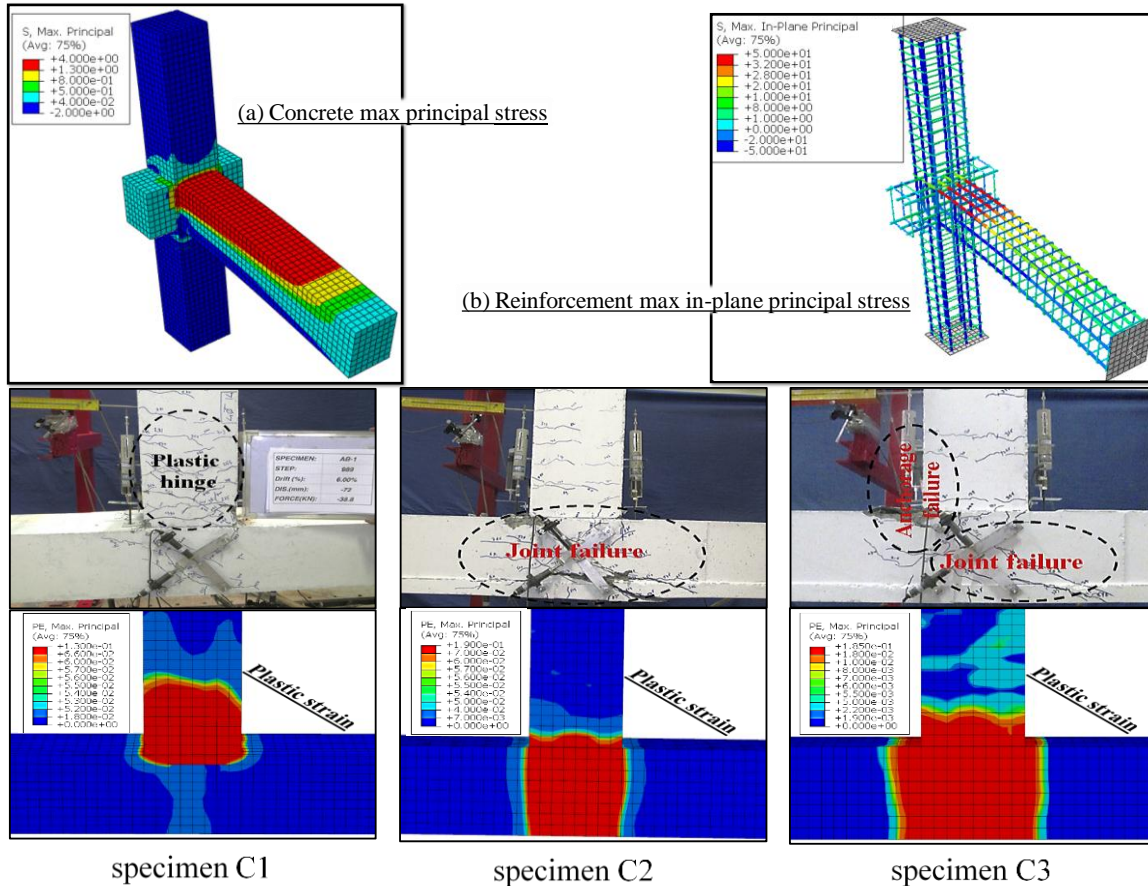


Figure 7. Damage and crack pattern and strain condition of reinforcement.



Table 5. Numerical Linear Maximum capacity Ratio to Laboratory Linear Maximum capacity and Related Displacement.

No.	Specimen	Loading direction	Peak load (kN)		Displacement at the yield point (mm)		Strength prediction	Displacement at 20% drop of peak load (mm)		Ductility factor		Average ductility factor	
			test	FEA	test	FEA	Error%	test	FEA	test	FEA	test	FEA
1	C1-1	Push	-41.90	-49.24	-20.93	-18.00	17.5	-72	-72	3.4	4.0	3.8	4.7
		Pull	36.40	38.55	17.33	13.33	5.9	72	72	4.2	5.4		
2	C2-1	Push	-37.10	-38.70	-18.00	-10.00	4.3	-54	-54	3.0	5.4	3.5	5.0
		Pull	31.30	35.38	13.33	12.00	13	54	54	4.1	4.5		
3	C3-1	Push	-40.75	-39.95	-22.00	-10.00	2	-52.75	-26.54	2.4	2.7	2.0	7.4
		Pull	21.20	19.59	14.67	2.67	7.6	23.83	32.56	1.6	12.2		
4	C1-1-S	Push	-41.90	-48.47	-20.93	-20.67	15.7	-72	-72	3.4	3.5	3.8	3.8
		Pull	36.40	37.99	17.33	17.33	4.4	72	72	4.2	4.2		
7	C2-1-S	Push	-37.10	-37.59	-18.00	-13.33	1.3	-54	-54	3.0	4.1	3.5	3.8
		Pull	31.30	34.78	13.33	14.93	11.1	54	54	4.1	3.6		
10	C3-1-S	Push	-40.75	-38.98	-22.00	-13.33	4.3	-52.75	-29.39	2.4	2.2	2.0	6.3
		Pull	21.20	18.74	14.67	4.00	11.6	23.83	41.80	1.6	10.5		

3.2. Effect of Transverse Beam

Results of Load - Displacement for different side beam conditions can be seen in Figure 8 . As shown, the amount of bearing load in the corner joints covered only by the beam in both sides is 2.5% and 6.8%, respectively, in the C1 and C2 specimens, respectively, in comparison with specimens without the presence of a cross beam. Be it. It also has a bearing load value of 0.5% and 6.2%, respectively, less than the joints covered by the beam in three sides. The influence of the presence of side beams on the load and absorption of energy indicates the confinement of these beams on the joint area. The confinement effect of presence of the transverse beam on the joint area can cause delaying the joint cracking. The side beam, as can be seen, does not affect the elastic stiffness of the structure, and in seismic-detail joints, without altering the stiffness, it only increases the plastic joint's capacity in the beam. In seismic detail defective joints, the flexural and shear capacity of the joint is increase. According to Table 6, the amount of load increased by the side beams in the C1, C2 and C3 joints (2.8%, 9.9% and 10.1%, respectively). In terms of seismic detail, it has not had a uniform effect. By comparing the three samples, it is observed that the confinement effect in C1, C2 and C3 samples increased, respectively. The confinement content of the side beams on one side and the side beams on the two side are 5.4% and 9.7%, respectively. The presence of confinement intensity difference in these three samples and the exponential difference of confinement of the middle and corner joints indicate that the impact of the confining area for a seismic detail without seismic detail has a 3% and 20% effect on the seismic behavior, respectively.

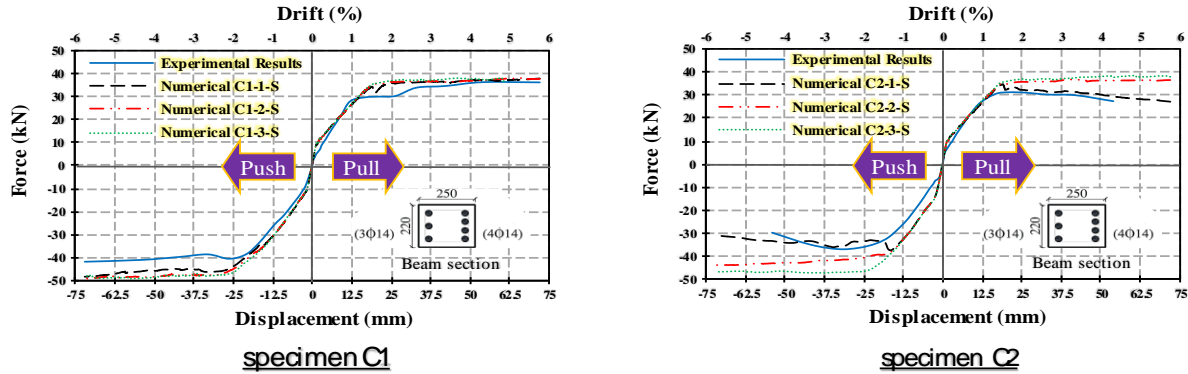


Figure 3. Load-displacement curve of specimen with different beam conditions and laboratory results.

Table 6. Maximum linear load with different transverse beam conditions and the percentage difference.

No.	Specimen	Loading direction	Peak load (kN),FEA	Percentage of force difference with specimen without lateral beam (%)
5	C1-2-S	Push	-49.68	2.5
		Pull	38.94	2.5
6	C1-3-S	Push	-49.92	3
		Pull	39.13	3
8	C2-2-S	Push	-41.35	10
		Pull	36.00	3.5
9	C2-3-S	Push	-45.11	20
		Pull	36.87	6
11	C3-2-S	Push	-42.88	10
		Pull	19.49	4
12	C3-3-S	Push	-46.78	20
		Pull	19.96	6.5

3.3. The Effect of Dilation Angle

Figure 9 shows that the model response is strongly dependent on the value of the dilation angle. The maximum load and displacement increased as the dilation angle increased. Figure 9 also shows that at the dilation angle value of 25 the convergence with other values is greater and closer to the experimental results. Therefore, this value was used for all models.

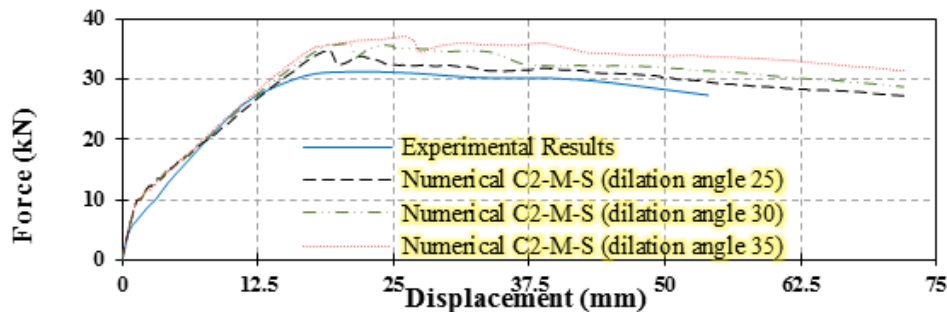


Figure 9. The effect of dilation angle on model C2-M-S.



4. Conclusion

In numerical modelling of reinforced concrete joints, indirect simulation of the effects of sliding longitudinal beam reinforcement on the beam-to-column joint area reduces the stiffness by 20% and is closer to the experimentally tested specimen's behaviour of 30% and more precisely can be investigated the complex behaviour RC beam-column joints. Numerical results obtained from models with seismic detail and non-seismic detail under different beam conditions confirmed that the greater the seismic weakness of the joint, the confinement the joint will have a greater impact on the damage recovery and the plastic resistance will increase. (3% to 20%), and further confining the joint area reduces the strength recovery, thus helping to achieve the desired pattern for the beam-to-column connections.

5. References

- [1]- Paulay, T., and Priestley, M. N., 1992, **Seismic design of reinforced concrete and masonry buildings**.
- [2]-Hawileh, R. A., Rahman, A., and Tabatabai, H., 2010, **Nonlinear finite element analysis and modeling of a precast hybrid beam–column connection subjected to cyclic loads**. Applied Mathematical Modelling, 34(9), 2562-2583. doi:<https://doi.org/10.1016/j.apm.2009.11.020>
- [3]-Roehm, C., Sasmal, S., Novák, B., and Karusala, R., 2015, **Numerical simulation for seismic performance evaluation of fibre reinforced concrete beam–column sub-assemblages**. Engineering Structures, 91, 182-196. doi:<https://doi.org/10.1016/j.engstruct.2015.02.015>
- [4]- Shafaei, J., Hosseini, A., and Marefat, M. S., 2014, **Seismic retrofit of external RC beam–column joints by joint enlargement using prestressed steel angles**, Engineering Structures 81, 265-288.
- [5]-Mander, J. B., Priestley, M. J., and Park, R. J., 1988, **Theoretical stress-strain model for confined concrete**, Engineering Structures, 114(8), 1804-1826.
- [6]-Genikomsou, A. S., and Polak, M. A., 2015, **Finite element analysis of punching shear of concrete slabs using damaged plasticity model in ABAQUS**, 98, 38-48.
- [7]-Alva, G. M. S., and de Cresce El, A. L., 2013, **Moment–rotation relationship of RC beam–column connections**, Experimental tests and analytical model. 56, 1427-1438.
- [8]-Lowes, L. N., Mitra, N., and Altoontash, A., 2003, **A beam-column joint model for simulating the earthquake response of reinforced concrete frames**.
- [9]-Monti, G., and Spacone, E. J., 2000, **Reinforced concrete fiber beam element with bond-slip**, Engineering Structures, 126(6), 654-661.
- [10]-Tan, K. H., & Yu, J., 2014, **Numerical analysis with joint model on RC assemblages subjected to progressive collapse**.
- [11]-Feng, D.-C., Wu, G., and Lu, Y., 2018, **Finite element modelling approach for precast reinforced concrete beam-to-column connections under cyclic loading**, Engineering Structures 174, 49-66.